On the impact of controlled surface roughness shape on the slippage of a soft-material
Slippage of soft-materials in rough microchannels

F. Pelusi[1], S. Sbragaglia[1], A. Scagliarini[2], M. Lulli[4], M. Bernaschi[2], and S. Succi[4,2]

[1]Dipartimento di Fisica, Università di Roma "Tor Vergata" and INFN - Via della Ricerca Scientifica 1, 00133 Rome, Italy
[2]Istituto per le Applicazioni del Calcolo CNR, via dei Taurini 19, Rome, Italy
[3]Department of Applied Physics, The Hong Kong Polytechnic University - Hung Hom, Kowloon, Hong Kong
[4]Center for Life Nano Science@La Sapienza, Istituto Italiano di Tecnologia, 00161 Roma, Italy

Abstract

We explore how geometrical corrugations change the near-wall flow properties of soft-materials confined in microchannels. By means of numerical simulations, we perform a quantitative analysis of scaling laws that relate the wall slippage to the wall stress σ_w. In particular, we address the importance of the roughness shape. Results show the existence of two regimes of slippage: a linear scaling $\sim \sigma_w$, for small stress values, and a quadratic one $\sim \sigma_w^2$, for large stress values. Interestingly, we find also that, while the two scaling laws are relatively robust, across different roughness realizations, for a given stress value, the slip-roughness relation depends on the geometry.

1 Introduction

Closely packed dispersions of soft particles are commonly encountered in industrial and every-day-life applications. Examples include concentrated emulsions, colloidal pastes, foams and gels [21, 10]. These "soft-materials" can sustain elastic deformations like solids do, and they are able to flow like non-Newtonian fluids for sufficiently large deformations, typically when the imposed stress exceeds a threshold value denoted as the "yield stress" [4, 7]. This rheological complexity lies at the root of the widespread use of such materials across many disparate fields, such as cosmetics [29], food processing [40], pharmaceutical products [20], oil recovery [9] and coatings [41] just to cite a few examples. Beyond the fundamental interest of understanding the microscopic mechanisms responsible for this rheological complexity [4, 7], another important issue arises when these materials flow close to a solid wall. In such conditions, the bulk rheological complexity is inevitably coupled to boundary effects [3, 8], and this coupling is more and more important at increasing confinement [18, 19, 23]. Typically, effective boundary conditions are introduced as a macroscopic manifestation of the microscopic interactions among soft particles and the wall. The most popular and studied boundary effect is probably *slippage* [28], i.e. the relative motion between the material and the wall confined in a thin boundary layer close to the wall. In the last two decades there has been a considerable effort to understand the physical mechanisms responsible for the slip of soft-materials with complex rheology, as recently reviewed in [8]. For smooth surfaces, one needs to distinguish two different regimes [26, 27, 36, 37], depending on whether the wall stress is below or above the yield stress. While above yield ("fluidized" regime) the slip is coupled to the bulk flow and is practically negligible for very large stresses, below the yield stress ("elastic" regime) the boundary slip dominates, while the soft-material moves as an elastic solid. In the elastic regime it has been shown that the slip depends on the particle-walls interactions [26, 27, 36, 37]. Specifically, when particles adhere to the surfaces, the slip velocity shows a quadratic scaling in the wall stress σ_w. When particles do not adhere to the solid surface the observed scaling between the slip velocity and the wall stress is typically linear [26, 27, 36, 37, 32, 2, 8]. In the fluidized regime, the situation is further complicated due to the coupling between the bulk flow and surface phenomena [18, 19]. In this context, various studies in the literature report scaling laws of the slip velocity as a function of the wall stress [34, 26, 27, 38, 15, 17, 19, 8, 37, 32, 24, 2, 33, 39, 1, 30]: while there are convincing indications that the packing fraction of the soft-material influences the scaling exponent [15], the non trivial role played by the particle-walls interactions is not clearly understood. Moreover, for soft-materials as foams, further enrichments are brought by the chemical properties of the surfactants used to stabilize the dispersion [11, 12, 25].
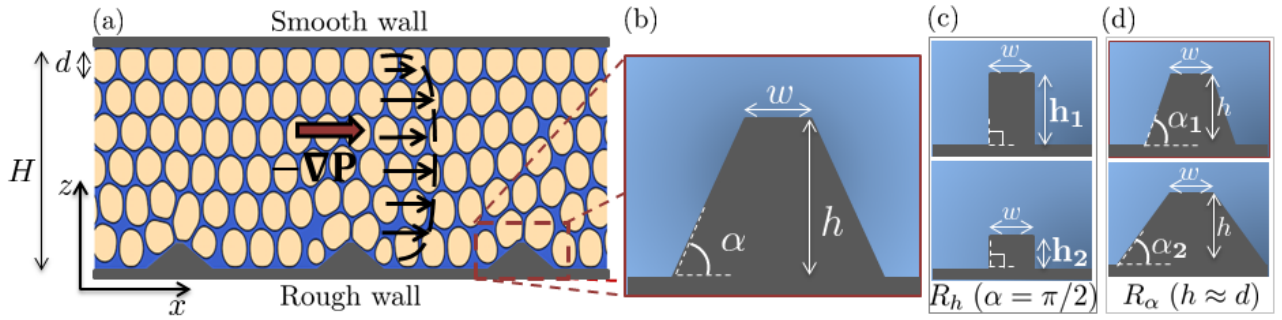
Figure 1: Set-up for the numerical simulations of soft-material through rough microchannels. Using lattice-Boltzmann simulations (see [35, 13, 14] and references therein) we prepare droplets of a dispersed phase (light yellow) packed together in a continuous phase (dark blue) (Panel (a)). Droplet size distribution is slightly polydisperse with an average diameter d. The soft-material is confined in a channel of width $H \approx 7d$ and driven with a constant pressure gradient along the stream-flow direction x. One wall of the channel comprises a regular roughness of equally spaced posts with trapezoidal shape (Panel (b)) with the height h and the angle α being the free parameters in our analysis, while the width w is kept fixed to the droplet scale, i.e. $w \approx d/3$. We analyze two roughness realizations: by varying h while keeping $\alpha = \pi/2$ (R_{h}, Panel (c)) and by varying α by keeping $h \approx d$ fixed (R_α, Panel (d)).

Another property of the surface that decidedly influences slippage is wall *roughness*. There is evidence from different studies in the literature that roughness changes the *wall fluidization* of the soft-material close to the walls [18, 19, 23, 17, 24, 31, 35, 13, 14]. Regarding slip, it is also commonly accepted that roughness suppresses it (see [8] and references therein). Some authors also reported that wall slippage scales differently with the wall stress when using a rough surface instead of a smooth surface [19]; however, reported data generically refer to the fluidized regime and systematic studies on how the wall slippage scales with the wall stresses for different wall roughness geometry are rather scarce. Naturally, this poses important questions: how does the roughness decrease wall slippage? Does the roughness shape matter? How are the scaling laws relating slippage to wall stresses changed by continuously increasing surface roughness? In this paper we aim at addressing these questions presenting a comprehensive analysis based on numerical simulations of a model soft-material driven by a constant pressure gradient in a confined channel. We will concentrate mainly on wall stress values below or of the order of the material yield stress, mainly because for smooth surfaces the slippage properties in this regime are well understood in terms of elasto-hydrodynamics and particle-wall interactions [26, 27, 36, 37, 8], hence we can draw a parallel with the phenomenology already exposed in the literature.

2 Numerical method and simulations setup

We resort to the lattice Boltzmann methodology (see [35, 13, 14] and references therein) to simulate a collection of droplets (see Fig. 1) packed together in a continuous phase and driven by a constant pressure gradient applied in the stream-flow (x) direction of a confined channel. The code is a variant of the original implementation described in [6] that takes full advantage of the huge computing power of modern Graphics Processing Units (GPU), making possible to run the very large number of simulations required by this kind of systematic study in a reasonable time on a small cluster equipped with multiple GPUs. The packing fraction of the droplets is large enough to produce a non vanishing yield stress. The droplet size distribution is slightly polydisperse with an average diameter d. Wetting properties are chosen in such a way that the droplets do not adhere to the walls, so as to fully expose the role of roughness [35, 13, 14]. Periodic boundary conditions are applied in the stream-flow direction, whereas two walls confine the system along the z direction: one wall ($z = H$) of the channel is flat, whereas the other ($z = 0$) is patterned with a periodic roughness comprising equally spaced posts of trapezoidal shape (see Fig. 1). This choice is instrumental to analyze two different realizations of the *roughness shape*: i) "varying-h"roughness with α fixed and equal to $\pi/2$ (roughness realization R_{h}); ii) "varying-α" roughness keeping h fixed to $h \approx d$ (roughness realization R_α). As a matter of fact, the roughness realization R_{h} is the most widely used and studied in the literature [18, 24, 35, 13, 14]. However, by thinking of a generic roughness profile $h(x)$, one could say that in the realization R_{h} the roughness results from different height variations "strongly" localized in space; hence, the natural complementary situation is that of a fixed height with variable localization in space, which motivates the choice of the realization R_α. Summarizing, the two roughness realizations are chosen in a complementary way so as to highlight both the importance of height variations as well as the roughness localization in space. Notice that in both realizations the roughness value
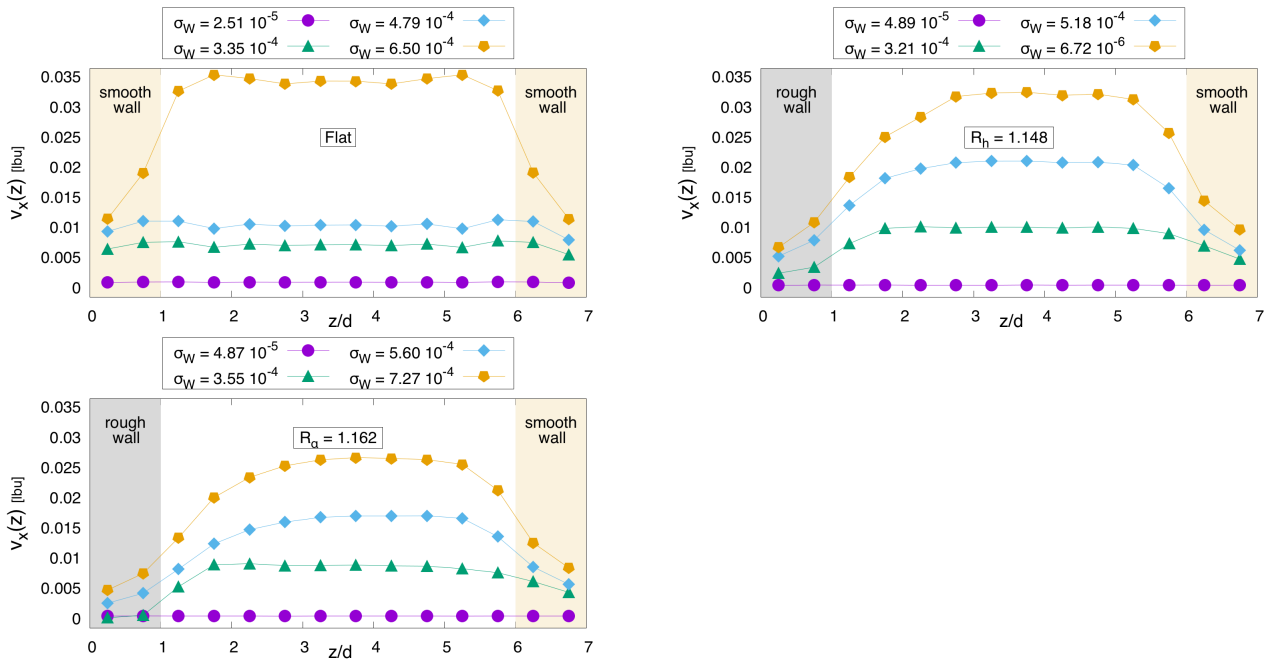
2

Figure 2: Velocity profiles for different values of rough-wall stress. Top panel: flat case. Central panel: rough case with realization R_h ($R_h = 1.148$). Bottom panel: rough case with realization R_α ($R_\alpha = 1.162$).
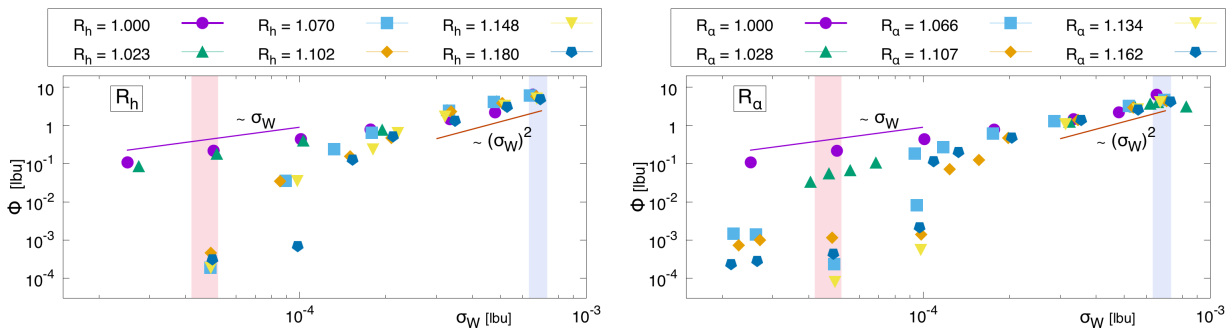

Figure 3: Log-log plot of the average mass flow-rate Φ as a function of the rough-wall stress σ_w for two different realizations of the roughness shape: R_h (top panel) and R_α (bottom panel). Relevant scaling laws are highlighted (see text for details). Shaded regions refer to two specific wall stress intervals later analyzed in Fig. 4.

R is obtained as the ratio between the real area of the rough surface and the projected one, so it is equal to unity for smooth walls. R increases with the height h in the realization R_h and with α in the realization R_α. From the methodological point of view, with respect to our previous investigations [35, 13, 14], the change in roughness shape is the added value brought by the present study. Given the roughness realization and value, the control parameter for the simulations is the pressure gradient, which is tuned so as to produce a value of wall stress σ_w below or of the order of the material yield stress. The wall stress is an outcome of the simulations and can only be measured a posteriori [5, 16], once the simulation has reached a steady state. We remark that by wall stress σ_w we indicate the stress in contact with the rough surface: this is the key observable required to obtain a fair assessment of the role that different roughness shapes play in the resulting slippage properties. To the purpose of running many simulations for different roughness shapes/values and wall stress values, we kept the wall-to-wall resolution fixed to $H \approx 7d$. All the results of the numerical simulations are reported in lattice Boltzmann units, hereafter lbu.

3 Results

The core of our results is displayed in Figs. 2 and 3. We average the instantaneous stream-flow velocity field along the stream-flow coordinate, x. The resulting velocity profiles, $v_x(z,t)$, are further integrated in z to obtain the instantaneous flow rate $\phi(t)$. Both the latter quantity and the velocity profiles $v_x(z,t)$ are, in
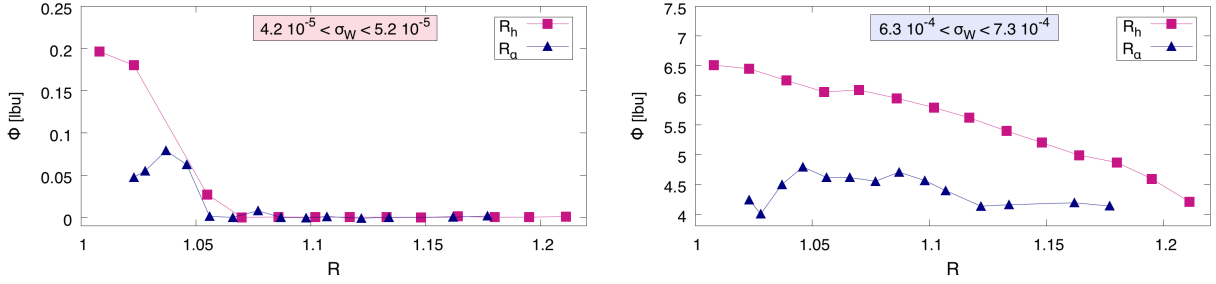
Figure 4: Mass flow-rate Φ as a function of roughness for two different roughness realizations R_{h} and R_{α} (see Fig. 1). The value of the wall stress σ_{w} is selected in two intervals (see also shaded areas in Fig. 3): $\sigma_{\mathrm{w}} \in [4.2 \, 10^{-5} : 5.2 \, 10^{-5}]$ ("small wall stress");$\sigma_{\mathrm{w}} \in [6.3 \, 10^{-4} : 7.3 \, 10^{-4}]$ ("large wall stress").

general, fluctuating quantities; in the following we will consider them as time average over the (statistically) steady state. The average mass flow-rate Φ is reported as a function of the rough-wall stress σ_{w} in Fig. 3 for both the realizations R_h (top panel) and R_α (bottom panel). Some velocity profiles $v_x(z)$ for both a flat case ($R_{\mathrm{h}} = R_\alpha = 1$) and the rough cases ($R_{\mathrm{h}} = 1.148$ and $R_\alpha = 1.162$) are displayed in Fig. 2 as a function of z/d. Since all the values of the rough-wall stresses are below or of the order of the yield stress of the soft-material, the velocity profiles essentially display a "plug dominance" in which the wall slip is the relevant contribution to the flow-rate (see Fig. 2). Only for the largest values of the wall stress, the velocity profiles display a bending strongly localized close to the walls, in a region having a width comparable to the mean droplet diameter. The emergence of regions with distinctive flow characteristics, *plug* and fluidized boundary layers, and the transition between them is sharper, hence neater, for the flat channel (top panel), whereas it is smoother for rough cases (central and bottom panel). Physically, these changes in the velocity profiles are generated by *boundary yielding events* of droplets of the bulk phase with respect to droplets that flow adjacent to the wall (boundary droplets). While for the flat channel (Fig. 2 top panel) such boundary yielding is symmetric, for the rough channel it is asymmetric [13, 14], with the yielding close to the rough wall ($z = 0$) more "vigorous" with respect to the flat wall case ($z/d = 7$). By assuming the boundary yielding process as responsible for setting an effective boundary condition, it is then mandatory to study the dependency of the slip (or the mass-flow rate) on the value of the rough-wall stress. This is done indeed in Fig. 3. For the sake of clarity we separately discuss *flat/weakly rough surfaces*[1] and *moderate/strongly rough surfaces*[2], being their phenomenology somehow different.

3.1   Flat/Weakly rough surfaces

It is apparent that the relation between Φ and σ_{w} exhibits two scaling-laws: while for small σ_{w} we observe a linear scaling-law, $\Phi \sim \sigma_{\mathrm{w}}$, for larger values of the wall stress a quadratic scaling-law ($\Phi \sim \sigma_{\mathrm{w}}^2$) is observed. For a soft-material whose "droplets" do not adhere to the boundary, Meeker and coworkers [26, 27, 37] already predicted and observed a linear scaling law for wall slippage as a function of the wall stress. This is confirmed by our numerical simulations. Nevertheless, our results support the view that this behaviour also persists for weakly rough surfaces. Regarding the quadratic scaling-law at larger values of the wall stress, we attribute it to the different physical mechanism setting the (effective) slip at the wall, i.e. the boundary yielding events described previously: boundary droplets act as a "soft mattress", which is elastically deformed up to the point where it yields, allowing the bulk droplets to sprint forward by developing a relative motion – hence dissipation – with respect to the boundary droplets. Under these conditions, we can think of a balancing between elastic deformation and viscous dissipation in the boundary region. Such balance, as already known from elasto-hydrodynamics studies [26, 27, 37], predicts a quadratic scaling-law of the boundary slip as a function of the wall stress.

3.2   Moderate/strongly rough surfaces

When the roughness further increases, we observe that for small values of σ_{w} the mass flow-rate drops essentially to zero, decreasing by 2-3 orders of magnitude, while data become more scattered, with a practical impossibility to make any clear statement about the presence of a scaling-law. At larger σ_{w}, instead, the drop in the flow-rate seems still present, but by no means comparable to what is observed at smaller σ_{w}. At intermediate values of the stress, a region of crossover appears, where the mass flow-rate passes from negligible values to non zero values and a quadratic scaling-law is recovered. In comparison with the flat/weakly rough surfaces, we observe

---

[1]For flat/weakly rough surfaces we mean a range of the roughness parameter R that goes from $R = 1.000$ (flat case) to $R = 1.030$.
[2]For moderate/strongly rough surfaces we mean a range of the roughness parameter R that goes from $R = 1.030$ to $R = 1.180$.

that the quadratic scaling-law region is broader, in that it starts at smaller values of wall stress. If we think of the quadratic scaling-law as a signature of boundary yielding events, this result is not surprising. Indeed, roughness has the tendency to block the droplets flowing adjacent to the boundary layer, hence it facilitates the yielding of the droplets of the bulk phase.

Overall, the picture outlined above is qualitatively unchanged for different roughness realizations. However, to support more quantitatively our results and to highlight more systematically the drops in the flow-rate that we observe at small and large values of rough-wall stress, we considered the wall stress in a given narrow interval and conducted simulations according to a fine grain tuning of the values of surface roughness. We selected two narrow intervals: i) "small wall stresses" ($\sigma_\mathrm{w} \in [4.2\,10^{-5} : 5.2\,10^{-5}]$) located well inside the region where the abrupt drop in the mass flow-rate is observed Fig. 3; ii) "large wall stresses" ($\sigma_\mathrm{w} \in [6.3\,10^{-4} : 7.3\,10^{-4}]$) located in the region where the quadratic scaling-law is observed in Fig. 3. In Fig. 4 we report the results for Φ as a function of the roughness value, for both roughness realizations and for the two intervals. Data for small wall-stresses (top panel) reveal that the drop to zero of the mass flow-rate is practically continuous; close to the critical roughness – where Φ becomes essentially zero – both realizations yield comparable values. Notice that the values of wall stresses considered in the top panel correspond to a situation where the material either advances as a plug or stops, i.e., no boundary yielding events are present. For large values (bottom panel), instead, a clear quantitative distinction between the two roughness realizations is observed: while Φ for R_h is monotonously decreasing, Φ for R_α appears rather constant. This tells us that under the conditions of an effective slippage induced by boundary yielding events, the blockage effect is mainly driven by the roughness height.

4   Conclusions

Summarizing, we have systematically analyzed the scaling properties of the mass flow-rate of a soft-material in a confined channel as a function of the wall-stress on the rough surface. To emphasize surface effects, we focused our attention only on values of the rough-wall stress below or of the order of the material yield stress. Hence, the major contribution to the mass flow-rate is essentially given by the slippage at the boundaries. We have considered the impact of roughness shape. To that purpose, we have designed two complementary roughness realizations, so as to highlight both the importance of height variations (R_h) as well as the roughness localization in space (R_α). Independently of the roughness shape, two different scaling laws are observed for flat/weakly rough surfaces: for small wall stresses the scaling-law is linear, whereas it crosses to a quadratic scaling at larger wall stresses. The crossover between the two scalings signals the presence of boundary yielding events strongly localized close to the boundary, which are clearly visible in the velocity profiles. An increase of the roughness parameter value suppresses the linear scaling, whereas the quadratic scaling still persists, on a broader interval. The main quantitative effect associated with the roughness shape pertains the drop in the mass flow-rate at large wall stresses, i.e. when boundary yielding events take place. In such situation, while the mass flow-rate for the realization R_h is a decreasing function of the roughness value, it stays practically constant for the realization R_α. These results indicates that the variation in height is mainly responsible for the drop in the mass-flow rate. Taken all together, we argue that these results may be useful for designing microfluidic channels to control and passively drive the motion of a soft-material. For future investigations, multiple pathways are worth being pursued. As already remarked in the introduction, the slippage characterization in the "solid" regime needs to be complemented with the corresponding characterization in the "fluidized" regime, where the surface properties are inevitably coupled to the bulk flow. In the spirit of the analysis already proposed in [15] for smooth surfaces, it would be interesting to quantitatively investigate the scaling laws above yield and the way they change in presence of roughness. In this regime, roughness inevitably triggers rearrangements [18, 19, 24, 31, 35, 13, 14] and could also be interesting to analyze the impact of roughness shape on such fluidization. In this work we focused on the time-averaged flow rate, which oscillates weakly in the "solid" regime. The flow rate fluctuations tend to grow as the transition to fluidization is approached. It is then logical to address how the amplitude and frequencies of these oscillations depend on the wall roughness geometry and how they correlate to the topological characteristics of the droplet assembly constituting the soft-material.

5   Acknowledgments

References

[1] F. Ahonguio, L. Jossic & A. Magnin, *AiChE J* **62**, 1356-1363 (2016)

[2] S. Aktas, D.M. Kalyon, B. M. Marin-Santibanez & J. P. Gonzalez, *Jour. Rheol.* (2014)

[3] H. A. Barnes, *J. Non-Newt. Fluid Mech.* **95**, 221 (1995)

[4] N. J. Balmforth, I. A. Frigaard, and G. Ovarlez, *Ann. Rev. Fluid Mech.* **46**, 121 (2014).

[5] M. Sbragaglia & D. Belardinelli, *Phys. Rev. E* **88**, 013306 (2013).

[6] M. Bernaschi, R. Benzi, L. Rossi, M. Sbragaglia & S. Succi, *Phys. Rev. E* **80**, 060103 (2009).

[7] D. Bonn, M. M. Denn, L. Berthier, T. Divoux & S. Manneville, *Rev. Mod. Phys.* **89**, 035005 (2017).

[8] M. Cloitre & R. Bonnecaze, *Rheol. Acta* **56**, 283-305 (2017)

[9] Chang, C., Q. D. Nguyen & H. Ronningsen, *J. Non-Newt. Fluid Mech.* **87**, 127 (1999)

[10] P. Coussot, Rheometry of Pastes, Suspensions, and Granular Materials (Wiley-Interscience, 2005).

[11] N.D. Denkov, V. Subramanian, D. Gurovich & A. Lips, *Colloids and Surfaces A: Physicochem. Eng. Aspects* **263**, 129-145 (2005)

[12] N. D. Denkov, S. Tcholakova, K. Golemanov, V. Subramanian & A. Lips, *Colloids and Surfaces A: Physicochem. Eng. Aspects* **282**, 329-347 (2006)

[13] L. Derzsi, D. Filippi, G. Mistura, M. Pierno, M. Lulli, M. Sbragaglia, M. Bernaschi & P. Garstecki, *Phys. Rev. E* **95**, 052602 (2017)

[14] L. Derzsi, D. Filippi, M. Lulli, G. Mistura, M. Bernaschi, M. Sbragaglia, P. Garstecki & M. Pierno, *Soft Matter* **14**, 1088-1093 (2018)

[15] T. Divoux, V. Lepeyre, V. Ravaine & S. Manneville, *Phys. Rev. E* **92**, 060301(R) (2015)

[16] B. Dollet, A. Scagliarini & M. Sbragaglia, *Jour. Fluid. Mech.* **766**, 556-589 (2015)

[17] B. Geraud, L. Bocquet & C. Barentin, *Eur. Phys. J. E* **36**, 30 (2013)

[18] J. Goyon, A. Colin, G. Ovarlez, A. Ajdari & L. Bocquet, *Nature* **454**, 84-87 (2008).

[19] J. Goyon, A. Colin & L. Bocquet, *Soft Matter* **46**, 2668 (2010)

[20] M. T. Islam, N. Rodriguez-Hornedo, S. Ciotti & C. Ackermann, *Pharmaceutical Research* **21**, 1192-1199 (2004)

[21] R. G. Larson, The Structure and Rheology of Complex Fluids (Oxford University Press, 1999).

[22] Z. Liu, M.A. Meyers, Z. Zhang and R.O. Ritchie, *Prog. Mater. Sci.* **88**, 467-498 (2017).

[23] V. Mansard & A. Colin, *Soft Matter* **8**, 4025 (2012).

[24] V. Mansard, L. Bocquet & A. Colin, *Soft Matter* **10**, 6984-6989 (2014)

[25] S. Marze, D. Langevin & A. Saint-Jalmes, *Jour. Rheol.* **52**, 1091-1111 (2008)

[26] S. P. Meeker, R. T. Bonnecaze & M. Cloitre, *Phys. rev. Lett.* **92**, 198302 (2004)

[27] S. P. Meeker, R. T. Bonnecaze & M. Cloitre, *Journal of Rheology* **48**, 1295 (2004)

[28] C. Neto, D. R. Evans, E. Bonaccurso, H.-J. Butt & V. S. J. Craig, *Rep. Prog. Phys.* **68**, 2859-2897 (2005)

[29] J. das Neves, M. V. da Silva, M. P. Goncalves, M. H. Amaral & M. F. Bahia, *Current Drug Delivery* **6**, 83-92 (2009)

[30] J. F. Ortega-Avila, J. Perez-Gonzalez, B. M. Marin-Santibanez, F. Rodriguez-Gonzalez, S. Aktas, M. Malik & D. M. Kalyon, *Jour. Rheol.* **60**, 503 (2016)

[31] J. Paredes, N. Shahidzadeh, and D. Bonn, *Phys. Rev. E* **92**, 042313 (2015).

[32] J. Perez-Gonzalez, J.J. Lopez-Duran, B.M Marin-Santibanez & F. Rodriguez-Gonzalez *Rheol. Acta* **51**, 937-946 (2012)

[33] A. Poumaere, M. M. Gonzalez, C. Castelain & T. Burghelea, *Jour. Non Newt. Fluid Mech.* **205**, 28-40 (2014)

[34] J.-B. Salmon, L. Becu, S. Manneville & A. Colin, *Eur. Phys. J. E* **10**, 209-221 (2003)

[35] A. Scagliarini, M. Lulli, M. Sbragaglia & M. Bernaschi, *Europhys. Lett.* **114**, 64003 (2016)

[36] J.-R. Seth, R. Bonnecaze & M. Cloitre, *Jour. Rheol.* **52**, 1241-1268 (2008)

[37] J.-R. Seth, C.-Locatelli-Champagne, F. Monti, R. Bonnecaze & M. Cloitre, *Soft Matter* **8**, 140 (2012)

[38] A.-L. Vayssade, C. Lee, E. Terriac, F. Monti, M. Cloitre & P. Tabeling, *Phys. Rev. E* **89**, 052309 (2014)

[39] B. D. Jofore, P. Erni, G. Vleminckx & P. Moldenaers, *Rheol. Acta* **54**, 581-600 (2015)

[40] G. Tabilo-Munizaga & G. V. Barbosa-Cánovas, *J. Food Eng.* **67**, 147 (2005)

[41] M. Maillard, C. Méziér, P. Moucheront, C. Courrier & P. Coussot, *J. Non-Newt. Fluid Mech.* **237**, 16-25 (2016)